3rd URSI AT-AP-RASC, Gran Canaria, 29 May – 3 June 2022

A Novel Faceted UTD Solver in Altair Feko for Antenna Placement Applications

Andres G. Aguilar (1), Lorena Lozano (2), Renier G. Marchand (3) and Ulrich Jakobus(1)
(1) Altair Engineering GmbH, Böblingen, Germany; e-mail aguilar@altair.com
(2) Department of Computer Science, University of Alcala, Madrid, Spain; e-mail: llozano@altair.com
(3) Altair Development, SA (Pty) Ltd, Stellenbosch, South Africa; e-mail: rmarchand@altair.com

Abstract

A new Faceted UTD solver as implemented in Altair Feko is introduced here. The solver is based on UTD (Uniform Theory of Diffraction) applied to planar and arbitrarily convex curved surfaces meshed with planar triangles. It is most suitable for antenna placement applications in the high frequency regime.

1. Introduction

Full wave solutions offer very accurate results, but problem size is limited by computational resources. PO (Physical Optics), RL-GO (Ray-Launching Geometrical Optics), and UTD are efficient high frequency methods that give accurate asymptotic results with much less effort (run-time, memory) for given classes of problems. UTD is very suitable for antenna placement applications. Modelling limitations in Altair Feko [1] and most other UTD codes are, however, present in the traditional UTD algorithms based on primitives such as flat polygonal plates and canonical circular cylinders. Faceted UTD is introduced in Altair Feko to overcome this limitation for antenna placement problems on planar and, more importantly, on generally convex curved surfaces using planar triangular meshes to represent the geometry as commonly used also for other electromagnetic solvers like MLFMM (Multilevel Fast Multipole Method). It is thus possible to calculate high frequency effects on a larger set of problems. Further hybridization of this Faceted UTD method with the MoM/MLFMM (anticipated as next step) allows the method to be used in even more complex scenarios.

2. Geometry representation and ray-tracing

The curvature properties of the geometry are calculated from the planar triangular mesh by using a quadratic interpolation between the vertices of connected triangles which ensures continuity of the interpolated surfaces across the triangle edges. This approach has the advantage that one can use a CAD model meshed with planar triangles without having to transform it to a different type of primitive, such as NURBS (Non-Uniform Rational B-Splines) [2], to represent the curvature of the geometry.

Several techniques have been used to accelerate the ray-tracing. Among others, two are worth mentioning. A kd-tree based space partitioning speeds up the ray-geometry occlusion tests [3] from any source or observer to the triangles. Moreover, an Angular Z-Buffer (AZB) [4] accelerates the visibility computations between triangles during the multiple interaction ray-path search. Additionally, Faceted UTD supports MPI parallel execution on multicore CPUs and clusters.

3. UTD field computation

The Faceted UTD includes the capability to compute from any impressed source direct and reflected ray effects [5] along with diffraction effects like edge/wedge diffraction [6], corner diffraction [7] and creeping rays [5]. Multiple reflections with one wedge diffraction at any position of the ray path are also supported. Other higher-order effects and concatenations of different ray effects will be added in the future.

When a source is close to the geometry, the ray-optical field approximations may not be accurate enough, as the exact field contains a radial field component at the interaction point that cannot be neglected and as higher order terms are present (not decaying with 1/r). To improve the accuracy of the Faceted UTD for antenna placement, a modified version of the UTD reflection coefficients has been used [8].

4. Examples

To show the capabilities of the Faceted UTD solver, we present simulations for canonical models and compare with a reference solution like MLFMM in Altair Feko. A more complex antenna placement scenario is also shown at the end.

Firstly, a PEC prolate spheroid illuminated by a $\hat{z}$-oriented infinitesimally small magnetic dipole is shown. The spheroid is centered at the global coordinate system and has a radius of curvature of $R_1 = 6\lambda$ and $R_2 = 12\lambda$, where $\lambda = 1\,\mathrm{m}$. The dipole is located at $(R_1 + \lambda, 0, 0)$ and has an amplitude of 1 Am^2. Faceted UTD uses 181 120 planar triangles for this model. Fig. 1 shows the electric near field

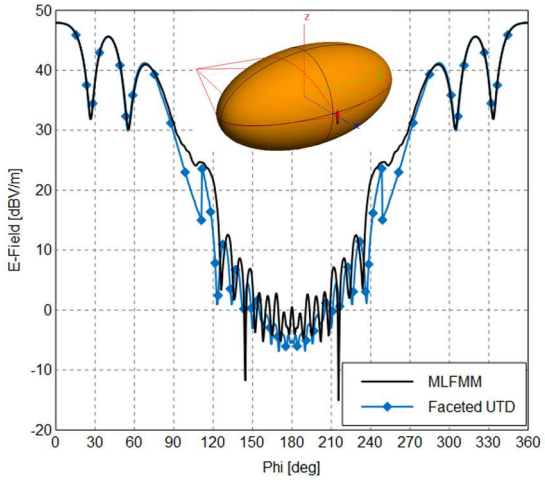

Figure 1. Electric near field of a magnetic dipole in front of a PEC prolate spheroid.

around the spheroid at $r = R_2 + 3\lambda\,, \theta = 90^o$ and $\phi \in [0°, 360°]$. with a sampling spacing of 0.5°. Between $\phi = 80° \ldots 80.5°$ (and analogously around $\phi = 279.5° \ldots 280°$), the transition region from the lit to the shadow region is found. Before that point, in the lit region, only direct and reflected rays are present, and afterwards, in the shadow region, only first order creeping rays are computed. One observes a uniform transition from the lit to the shadow region, as expected with UTD. The discontinuity around 111.5° is due to the transition from two to four first order creeping rays found. Moreover, the agreement with MLFMM is reasonably good.

The model in Fig. 2 is a reproduction of a model as shown in [7], with the important difference that, in our case, the truncated cylinder is not infinitely long on the $-\hat{z}$-axis, but has a length of 5λ. The model is a PEC truncated cylinder with a cross section defined by a Tschirnhausen cubic curve, whose parametric equations are $x = 3a(t^2 - 3)$ and y= $at(t^2 - 3)$, with $a = \lambda$ and $-\sqrt{3} \leq t \leq \sqrt{3}$), and it is closed at the cusp point $x = y = 0$ for $t = \pm\sqrt{3}$. The cylinder is truncated at $z = 0$ and $z = -5\lambda$. The truncated cylinder is illuminated by a $\hat{y}$-oriented infinitesimally small electric dipole, located at $(-4\lambda, -4\lambda, 4\lambda)$ and with an amplitude of 1 Am. The near field is sampled at $r = 2\lambda\,, \phi = 0$ and $\theta \in [-90°, 180°]$ with 501 points. The mesh for Faceted UTD contains 36 586 planar triangles. The results in Fig. 2 clearly show the correction near and within the Shadow Boundary Cones (SBCs) due to the addition of corner diffraction. The agreement between Faceted UTD with corner diffraction and the reference solution with MLFMM is quite good. The discontinuity around $\theta = 8.8°$ is due to the aforementioned finite length and can only be removed if other higher-order effects such as double wedge diffraction are included. The discontinuities around $\theta = 62.1°$ and 139.2° occur due to discrepancies between the CAD model and the interpolated mesh.

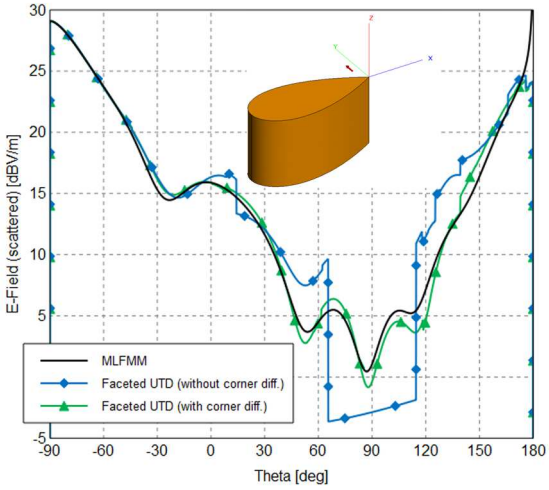

Figure 2. Electric near field (scattered field only) of an electric dipole near a PEC truncated cylinder with a Tschirnhausen cubic curve profile as used in [6].

In third place, two PEC parallel square plates illuminated by an electric dipole are simulated to show the multiple effects capabilities of Faceted UTD. Both plate dimensions are 1 m × 1 m with a frequency of 1 GHz, and are centered in $x = y = 0$. The bottom plate lays at $z = 0$ and the top one at $z = 0.5$ m. In this case, just two planar triangles per plate are enough to represent the geometry with Faceted UTD. The dipole is oriented along $\hat{z}$-axis, is located at (0,0,1.25) m. and has a source amplitude of 1 Am. Fig. 3 shows the electric near field along a line, $x = 0$, $z = 0.25$ m. and $y \in [-0.5, 0.5]$ m. with a sampling spacing of 0.02 m. This is a line between the two plates. The observation points are thus in the shadow region, where contributions are from wedge diffraction (first order interaction) but also from the wedge diffraction followed by multiple reflections within the inner plate sides (higher-order interactions or multiple effects concatenated). It can be seen in Fig. 3 that a better agreement with MLFMM is achieved if multiple or higher-order effects are included in the simulation. The discrepancies around $y = 0$ are probably due to the lack of other higher-order effects like double wedge diffraction, which will be added to Faceted UTD soon.

Finally, Fig. 4 shows a more complex antenna placement problem. This is a spherical mode source acting as an equivalent source of an antenna, located very close to the surface of a PEC helicopter. The frequency is 1GHz, which means the source is about 0.08λ away from the geometry surface. The helicopter spans approximately $51\lambda \times 17\lambda$. The total gain is measured on a circular scan for $\phi = 0$ and $\theta \in [-180°, 180°]$ with an angular increment of 1°. The agreement with MLFMM is reasonably good and the speed obtained with Faceted UTD, see Table I, is very good, with the advantage of being able to go up in frequency without any runtime or memory penalty if the mesh stays the same.

Table I summarizes the runtime and memory consumed by all the models considered in this paper. All models were run with an Intel Xeon CPU E5-2667 v4 3.20 GHz and with 4 cores.

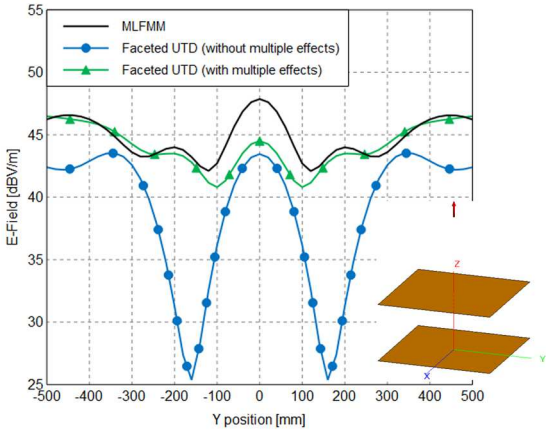

Figure 3. Electric near field of an electric dipole on top of two parallel square plates. The electric near field is sampled in between the two plates. In this case, multiple effects refers to wedge diffraction followed by multiple reflections.

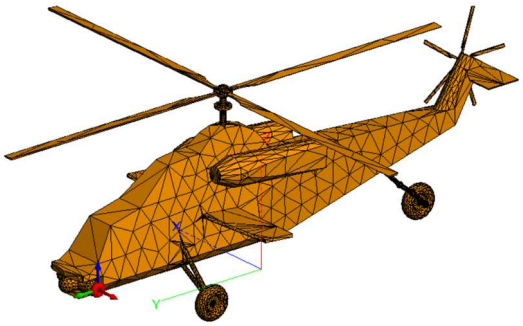

(a)

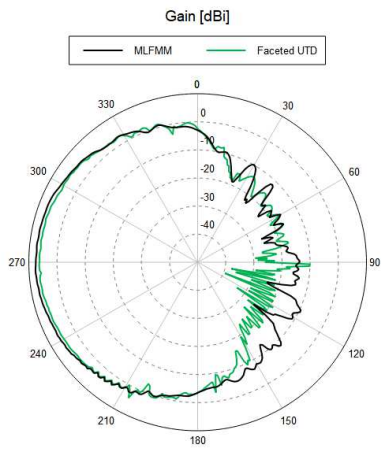

(b)

Figure 4. (a) Helicopter model with an spherical mode source and mesh for Faceted UTD. (b) Total gain at 1 GHz.

Table I. Summary of runtime and memory of the models run.

Model	*Runtime*		*Memory*	
	MLFMM	*Faceted UTD*	*MLFMM*	*Faceted UTD*
Spheroid	596.19 sec.	57.74 sec.	10.533 GByte	4.148 GByte
Truncated cylinder	111.29 sec.	25.8 sec.	1.972 GByte	218.88 MByte
Parallel plates	2.38 sec.	0.05 sec.	253.006 MByte	267.81 kByte
Helicopter	50.22 min.	3.06 sec.	3.240 GByte	226.67 MByte

References

[1] Altair Feko, Altair Engineering, Inc., https://www.altair.com/feko.

[2] J. Perez, J.A. Saiz, O.M. Conde, R.P. Torres, and M.F. Catedra, "Analysis of Antennas on Board Arbitrary Structures Modeled by Nurbs Surfaces", *IEEE Transactions on Antennas and Propagation*, vol. 45, no. 6, pp. 1045-1053, Jun. 1997.

[3] Y. B. Tao, H. Lin, and H. J. Bao, "KD-Tree based fast ray tracing for RCS prediction", *Progress In Electromagnetics Research*, vol. 81, pp. 329-341, 2008.

[4] M.F. Catedra, J. Perez, F. Saez de Adana and O. Gutierrez, "Efficient Ray-Tracing Techniques for Three-Dimensional Analyses of Propagation in Mobile Communications: Application to Picocell and Microcell Scenario", *IEEE Antennas and Propagation Magazine*, vol. 40, pp. 15-28, Apr. 1998.

[5] P.H. Pathak, W.D. Burnside, and R.J. Marhefka, "A Uniform GTD Analysis of the Diffraction of Electromagnetic Waves by a Smooth Convex Surface", *IEEE Transactions on Antennas and Propagation*, vol. AP-28, no. 5, pp. 631-642, Sep. 1980.

[6] R.G. Kouyoumjian, and P.H. Pathak, "A Uniform Geometrical Theory of Diffraction for an Edge in a Perfectly Conducting Surface", *Proceedings of the IEEE*, vol. 62, no. 11, pp. 1448-1461, Nov. 1974.

[7] M. Albani, G. Carluccio, and P.H. Pathak, "A Uniform Geometrical Theory of Diffraction for Vertices Formed by Truncated Curved Wedges", *IEEE Transactions on Antennas and Propagation*, vol. 63, no. 7, pp. 3136-3143, Jul. 2015.

[8] I.P. Theron, D.B. Davidson, and U. Jakobus, "Extensions to the Hybrid Method of Moments/Uniform GTD Formulation for Sources Located Close to a Smooth Convex Surface", *IEEE Transactions on Antennas and Propagation*, vol. 48, no. 6, pp. 940-945, Jul. 2000.